

# Linear simulation of ion temperature gradient driven instabilities in W7-X and LHD stellarators using GTC

Hongyu Wang,<sup>1</sup> Zhihong Lin,<sup>1,2</sup> Ihor Holod,<sup>2</sup> Jian Bao,<sup>1,2</sup> Lei Shi,<sup>2</sup> and Sam Taimourzadeh<sup>2</sup>

<sup>1</sup>*Fusion Simulation Center, Peking University, Beijing 100871, China*

<sup>2</sup>*Department of Physics and Astronomy, University of California, Irvine, California 92697, USA*

## Abstract

The global gyrokinetic toroidal code (GTC) has been recently upgraded to do simulations in non-axisymmetric equilibrium configuration, such as stellarators. Linear simulation of ion temperature gradient (ITG) driven instabilities has been done in Wendelstein7-X (W7-X) and Large Helical Device (LHD) stellarators using GTC. Several results are discussed to study characteristics of ITG in stellarators, including toroidal grids convergence, nmodes number convergence, poloidal and parallel spectrums, and electrostatic potential mode structure on flux surface.

## I. INTRODUCTION

After stellarators being designed in 1950s, several concepts in magnetic confinement devices are first presented in stellarators [reference1] and recently increasing attentions have been put on magnetic confinement devices with symmetry-breaking effects [reference2]. The non-axisymmetric feature in toroidal direction of stellarator brings many unique physical phenomenons and possible method of nuclear fusion. At the same time, considering the common properties of tokamak and stellarator, like new classical transport and Alfvén eigenmodes, research achievements of plasma physics in stellarators also help deeper understanding of tokamaks [reference3]. Several experimental results in stellarators have been received. W7-X, the biggest stellarator in the world currently, first produced helium plasma in December 2015 [reference4]. LHD firstly produced plasma in 1998 [reference5 6] and nowadays plasma confinement properties of LHD are comparable to world's fusion devices. Characteristics of micro turbulence have been studied in H-mode plasma in LHD [reference7], and inward radial propagation of spontaneous toroidal flow have been observed in LHD [reference8].

As stellarator is one kind of hopeful devices to make nuclear fusion come true, it is necessary to study characteristics of plasma physics in stellarators in both experiments and computer simulations. Several efforts have been put into simulations on stellarators. EUTERPE, a global particle-in-cell code, has been used to study the effects of collisions on ITG in LHD [reference9] and radial electric fields effects on linear ITG in W7-X and LHD [reference10]. GENE has done nonlinear simulation of ITG turbulence in W7-X [reference11] and compared simulation results of microinstabilities and turbulence with EUTERPE [reference12]. Linear simulations of ITG instabilities have also been studied for both standard and inward-shifted LHD configurations using GKV code [reference13], and an upgraded code, GKV-X, has done linear simulations of ITG using precise magnetic configurations of LHD, and comparisons between linear simulation results of ITG using GKV-X and LHD experiments observations are also given [reference14].

Recently, the global gyrokinetic toroidal code (GTC) has been upgraded to use 3D equilibrium

geometry and study plasma phenomenons in stellarators caused by non-axisymmetric equilibrium configurations. GTC is a global gyrokinetic particle-in-cell code [reference15], and a field-aligned magnetic coordinate  $(\psi, \theta, \zeta)$  is employed in GTC to represent magnetic fields and profiles of equilibrium quantities. To build realistic magnetic configurations, Variational Moments Equilibrium Code (VMEC) [reference16] is used in GTC. In this article, ion temperature gradient (ITG) instabilities in W7-X and LHD are explored using GTC and the simulations are all done in full torus. Effects of parallel grids and different modes coupling in W7-X and LHD on growth rates and real frequencies are investigated. Electrostatic potential on flux surface and 3D mode structures are also presented to study common characteristics and differences of ITG in W7-X and LHD.

The remainder of this paper is as follows. The method to upgrade GTC and construct non-axisymmetric magnetic fields using VMEC is presented in Section II. In Section III, simulation results of ITG in W7-X are given. Parallel grids convergence and Nmode convergence are studied to explore unique features caused by field periods of W7-X in parallel direction. Electrostatic potential on flux surface is plotted in  $(\theta, \zeta)$  space and 3D space to show mode structure directly. In section IV, simulation results of ITG in LHD are presented. Considering different technical structures of LHD and W7-X, parallel grids convergence, Nmode convergence, and mode structures are also studied in LHD. Conclusion and discussion are provided in Section V.

## II. CONSTRUCT NON-AXISYMMETRIC MAGNETIC FIELDS USING VMEC

Thanks to the collaboration between the GTC team at UCI and Spong at ORNL, GTC has recently been updated to treat 3D equilibria by interfacing with the MHD equilibrium code VMEC [reference11]. The equilibrium geometry and magnetic field data from VMEC is provided in the form of Fourier series coefficients  $B_{cn}$ ,  $B_{sn}$  in the toroidal direction:

$$B(\psi, \theta, \zeta) = \sum_{n=1}^N \left[ B_{cn}(\psi, \theta, n) \cos(ntor(n)\zeta_n) + B_{sn}(\psi, \theta, n) \sin(ntor(n)\zeta_n) \right] \quad (1)$$

where  $(\psi, \theta, \zeta)$  are normalized poloidal flux, poloidal angle, and toroidal angle, respectively, forming right-handed Boozer coordinate system,  $N$  the total number of toroidal harmonics chosen, and  $ntor(n)$  the corresponding toroidal harmonic mode number. The Fourier coefficients  $B_{cn}$  and  $B_{sn}$  are specified on a regular rectangular mesh on the  $(\psi, \theta)$  space, with the number of grid points  $(lsp, lst)$ . The magnetic field  $\zeta$ -dependence is essential in the stellarators, and is taken into account in the particle dynamics, gyrokinetic equation, and electron continuity equation in GTC.

Similar to the magnetic field strength  $B$ , the cylindrical coordinates  $(X, Z)$  are also given in the form of Eq. (1).

In addition, the flux functions representing poloidal  $g(\psi)$  and toroidal  $I(\psi)$  currents, effective minor radius  $r(\psi)$ , and magnetic safety factor  $q(\psi)$ , are provided.

We use quadratic spline interpolation along  $(\psi, \theta, \zeta)$  to efficiently evaluate the 3D equilibrium quantities. The spline coefficients are constructed on the identical mesh in  $(\psi, \theta)$  as the read-in VMEC data, and the same as the simulation grid along  $\zeta$ . The periodicity of the value and the first derivative in  $\theta$  and  $\zeta$  directions is enforced by using periodic boundary condition when constructing the spline. An odd number of spline sections in these directions is required due to intrinsic constraints of periodic quadratic spline [reference17].

### III. SIMULATION OF ITG IN W7-X

In a stellarator, both device configuration and produced plasma are not axisymmetric in toroidal direction anymore, and the cross sections of stellarator change at different toroidal angles. Poloidal contours look the same only after rotating a stellarator at certain angles in toroidal direction. Field period,  $N_{fp}$ , is used to describe this non-axisymmetric feature in stellarators, and it gives the rotating toroidal angle needed to make the poloidal contours looking the same. For W7-X, field period is 5 and it means the same cross sections of W7-X will be found through a minimum angle

of  $72^\circ$  in toroidal direction. The 2D poloidal contours at  $\zeta = \frac{0}{N_{fp}}, \frac{0.5\pi}{N_{fp}}, \frac{\pi}{N_{fp}}, \frac{1.5\pi}{N_{fp}}$  on

diagnosis flux surface of W7-X are given in FIG1.

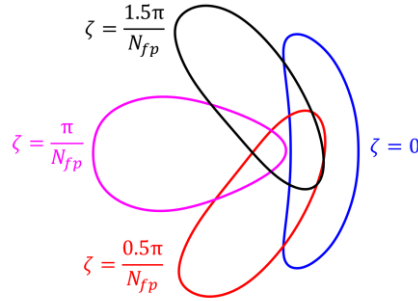


Figure 1. 2D poloidal contours of W7-X on diagnosis flux surface at  $\zeta=0$  (blue),  $\zeta=0.5\pi/N_{fp}$  (red),  $\zeta=\pi/N_{fp}$  (magenta) and  $\zeta=1.5\pi/N_{fp}$  (black).  $N_{fp}$  is field period and  $N_{fp}=5$  in W7-X.

Rotational transform is used to present magnetic field line traveling angles in toroidal and poloidal direction in stellarators and  $t=1/q$ , while  $q$  is safety factor in tokamaks. Ion temperature profile, in which ion temperature gradient  $\eta$  is 1, and rotational transform profile are given in FIG2(a). Simulation range of  $\psi$  is also marked out in FIG2, and diagnosis point is at  $\psi=0.5$ . Basic parameters used in simulations of W7-X are as follows: magnetic field on axis is 23600 Gauss, ion temperature at diagnosis point is 1000 eV, major radius is 561.79 cm,  $k_{\perp}\rho_i=0.0089$ , time step is 0.01 Cs/R0, and Cs/R0 is 2.43E-04. Growth rates and real frequencies of simulations in this section are normalized to Cs/R0. As introduced in Section I, Fourier series coefficients in  $\zeta$  expansion are used to build 3D magnetic field in GTC. Harmonic series  $ntor(n)$  is an arithmetic progression with common difference of 5, so the first 4 harmonic Fourier series  $ntor$  are 0, 5, 10,

15. The first 4 Fourier series coefficients  $B_{cn}(\psi, 1, 1)$ ,  $B_{cn}(\psi, 1, 2)$ ,  $B_{cn}(\psi, 1, 3)$ ,

$B_{cn}(\psi, 1, 4)$  used to construct 3D magnetic field of W7-X are given in FIG2(b).

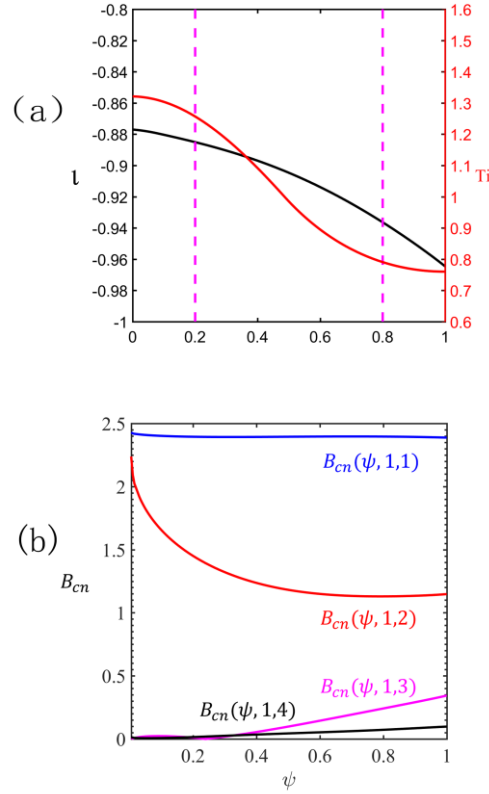


Figure 2. (a) Ion temperature (red) profile and rotational transform (black) profile. Simulation range is marked out by magenta lines:  $\psi_{\text{inner}}=0.2$  and  $\psi_{\text{outer}}=0.8$ . (b) Fourier series coefficients of magnetic field of W7-X used in GTC,  $B_{cn}(\psi, 1, 1)=0$  (blue),  $B_{cn}(\psi, 1, 2)=5$  (red),  $B_{cn}(\psi, 1, 3)=10$  (magenta),  $B_{cn}(\psi, 1, 4)=15$  (black). Values of  $B_{cn}(\psi, 1, 2)$ ,  $B_{cn}(\psi, 1, 3)$ ,  $B_{cn}(\psi, 1, 4)$  are multiplied by 10.

Considering non-axisymmetric equilibrium of W7-X, it is important to study parallel grids needed in simulations. Growth rates and real frequencies of  $n_{\text{mode}}=185$ ,  $m_{\text{mode}}=205$  when parallel grids  $N_p=17, 33, 65$ , and  $97$  are shown in FIG3. Parallel spectrums for different parallel grids are given in FIG4. According to growth rates, real frequencies and parallel spectrums, 65 parallel grids are needed to do full torus simulations in W7-X using GTC. As the coordinate of GTC is field-aligned, parallel grids needed are smaller to get convergence and it saves the computing resource greatly.

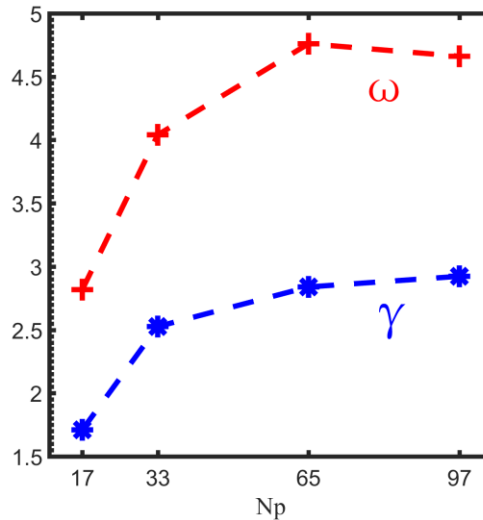


Figure 3. Growth rates (blue) and real frequencies (red) of parallel grids convergence.

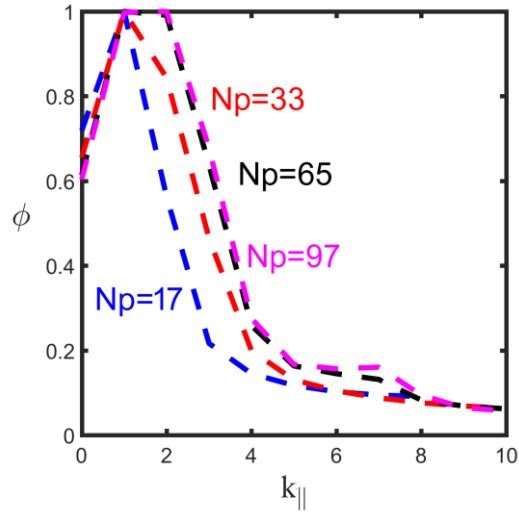


Figure 4. Parallel spectra of different parallel grids.

In GTC, after solving fields, a filtering step is put before gathering particles, so nmodes number. Nmode, can be set by choosing whether doing filtering. To study different modes coupling effects in W7-X, convergence of nmodes number also should be done. In simulations, one nmode, 3 nmodes, 7 nmodes and all nmodes are kept to study convergence of nmodes number convergence. When keeping only one nmode, all nmodes except nmodes=185 are filtered out. As filed period of W7-X is 5, nmodes=180, 185, 190 are kept when Nmode=3, and nmodes=170, 175, 180, 185, 190, 195, 200 are kept when Nmode=7. When keeping all nmodes in simulation, filtering step is omitted. Growth rates and real frequencies of nmode=185, mmode=205 are shown in FIG5.

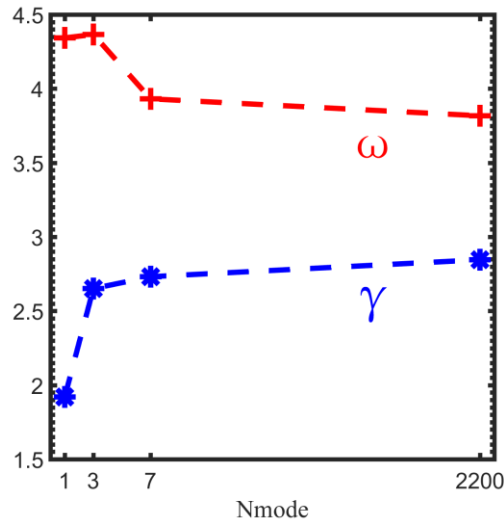


Figure 5. Growth rates (blue) and real frequencies (red) of Nmode convergence.

Growth rates and real frequencies of nmode=185 at different ion temperature gradients  $\eta$  are given

in FIG6, and  $\eta$  is defined as  $\eta = -\frac{d\ln Ti}{d\psi_{tor}}$ . In these cases, 3 nmodes are kept in simulations. These growth rates and real frequencies show good linearity with ion temperature gradient and are compared with simulation results of EUTERPE.

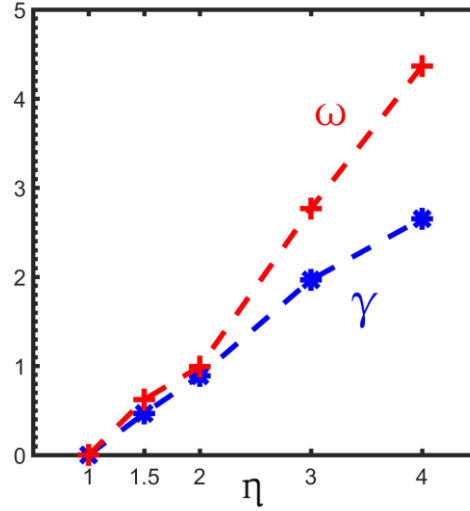


Figure 6. Growth rates (blue) and real frequencies (red) of nmode=185 and mmode=205 when keeping 3 nmodes in simulation.

Fast Fourier Transform Algorithm is used to calculate poloidal spectrum on flux surface. An average poloidal spectrum of diagnosis flux surface and other 10 flux surfaces, which are closet to diagnosis flux surface, is given in FIG7. Peak value of poloidal spectrum appears at around mmode=400.

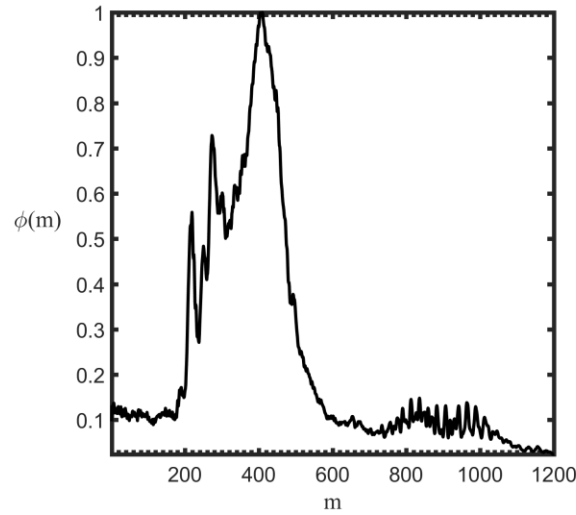


Figure 7. Averaging poloidal spectrum.

Electrostatic potential  $\phi$  on diagnosis flux surface is given in FIG8. X axis is  $\zeta$ , changing from 0 to  $2\pi$ , and y axis is  $\theta$ , changing from  $-\pi$  to  $\pi$ . It shows 5 up-and-down clusters in  $(\zeta, \theta)$  space. 3D mode structure of electrostatic potential on diagnosis flux surface is given in FIG9. They show the discrete toroidal symmetry of W7-X and reflect 5 field periods' effects. The mode structures repeat after rotating one field period, but still exit difference on potential intensity.

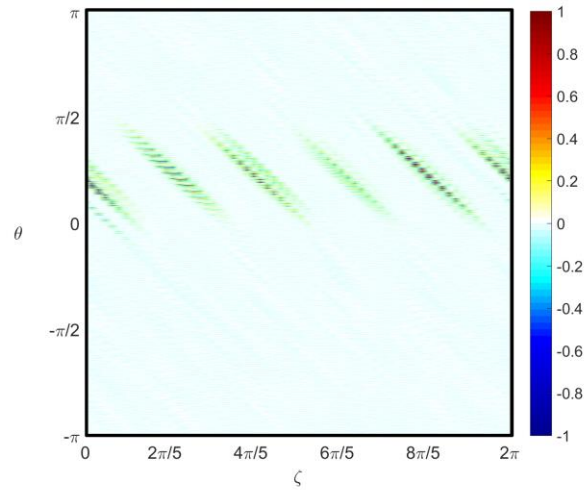


Figure 8. Phi on flux surface when keeping all nmodes. X axis is  $\zeta$  and y axis is  $\theta$ .

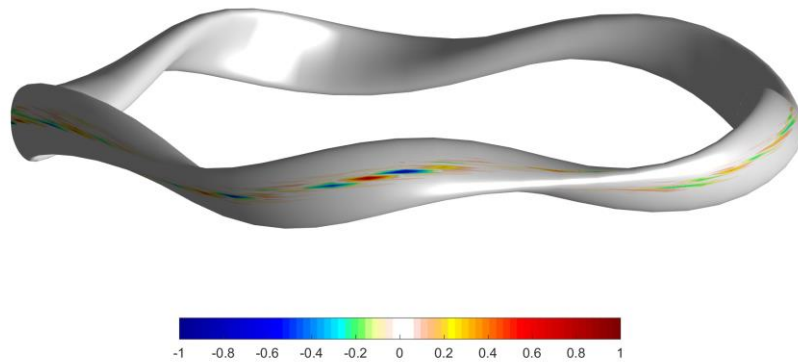


Figure 9. 3D electrostatic potential mode structure of W7-X.

#### IV. SIMULATION OF ITG IN LHD

For LHD, device configuration is different from that of W7-X. In LHD, field period  $N_{fp}$  is 10, and

2D poloidal contours at  $\zeta = \frac{0}{N_{fp}}, \frac{0.5\pi}{N_{fp}}, \frac{\pi}{N_{fp}}, \frac{1.5\pi}{N_{fp}}$  on diagnosis flux surface are given in

FIG10. Ion temperature and rotational transform profiles used in simulation of LHD are presented in FIG11(a), and simulation range of  $\psi$  is marked out and diagnosis point is at  $\psi=0.375$ . Basic parameters are as follows: magnetic field on axis is 14457.83 Gauss, ion temperature on axis is 1000 eV, major radius is 372.8 cm,  $k_{\perp}\rho_i=0.0098$ , time step is 0.004 Cs/R0, and Cs/R0 is 5.98E-04. Growth rates and real frequencies are normalized to Cs/R0 in this section. Fourier series coefficients in  $\zeta$  expansion are also used in LHD, like the method to build magnetic field of W7-X.

The first 4 Fourier series coefficients profiles  $B_{cn}(\psi,1,1)$ ,  $B_{cn}(\psi,1,2)$ ,  $B_{cn}(\psi,1,3)$ ,

$B_{cn}(\psi,1,4)$  used to construct 3D magnetic field of LHD are given in FIG11(b), and in LHD,

Fourier series  $ntor(n)$  is an arithmetic progression with common difference of 10 due to its field period, and the first 4 harmonic Fourier series  $ntor(n)$  are 0, 10, 20, 30.

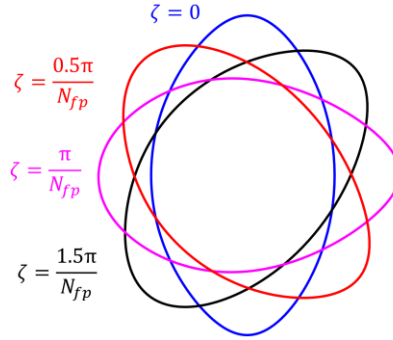


Figure 10. 2D poloidal contours of LHD on diagnosis flux surface at  $\zeta=0$  (blue),  $\zeta=0.5\pi/N_{fp}$  (red),  $\zeta=\pi/N_{fp}$  (magenta) and  $\zeta=1.5\pi/N_{fp}$  (black).  $N_{fp}=10$  in LHD.



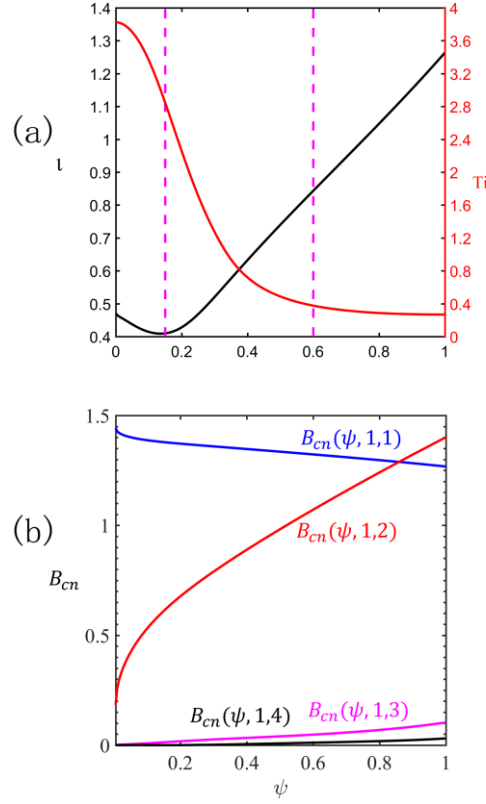


Figure 11. (a) Ion temperature (red) and rotational transform (blue) profiles. Simulation range is marked out by magenta lines:  $\psi_{\text{inner}}=0.15$  and  $\psi_{\text{outer}}=0.6$ . (b) Fourier series coefficients to build magnetic field of LHD in GTC,  $B_{cn}(\psi, 1, 1)=0$  (blue),  $B_{cn}(\psi, 1, 2)=5$  (red),  $B_{cn}(\psi, 1, 3)=10$  (magenta),  $B_{cn}(\psi, 1, 4)=15$  (black). Values of  $B_{cn}(\psi, 1, 2)$  and  $B_{cn}(\psi, 1, 3)$  are multiplied by 5. Values of  $B_{cn}(\psi, 1, 4)$  are multiplied by 20.

Considering field period of LHD is 10, more parallel grids are needed in simulations of LHD than W7-X. Parallel grids are set as 81, 121, 161, and growth rates and real frequencies of  $n_{\text{mode}}=37$ ,  $n_{\text{mode}}=61$  are given in FIG12. For LHD, 121 grids in parallel direction are necessary to get convergence in full torus simulations of LHD. According to parallel grids convergence of W7-X and LHD, 12 or more toroidal grids are needed for every field period of stellarators using GTC. Influences of modes coupling on growth rates and real frequencies in LHD are also studied. Applying the same analysis method like in W7-X, one  $n_{\text{mode}}$ , 3  $n_{\text{modes}}$ , 7  $n_{\text{modes}}$  and all  $n_{\text{modes}}$  are kept in four cases by adding a filtering step. For one  $n_{\text{mode}}$  case,  $n_{\text{mode}}=37$  is kept. For  $N_{\text{mode}}=3$ ,  $n_{\text{modes}}=27, 37, 47$  are kept, and for  $N_{\text{mode}}=7$ ,  $n_{\text{modes}}=7, 17, 27, 37, 47, 57, 67$  are kept. Growth rates and real frequencies of  $n_{\text{mode}}=37$ ,  $n_{\text{mode}}=61$  are calculated and presented in FIG13. Results show that growth rates and real frequencies of different  $n_{\text{modes}}$  coupling does not differ a lot in LHD, and the maximum value and the minimum value differs about 4%.

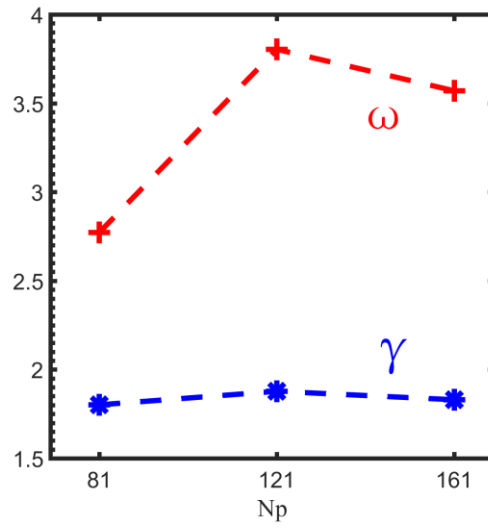


Figure 12. Growth rates (blue) and real frequencies (red) of parallel grids convergence.

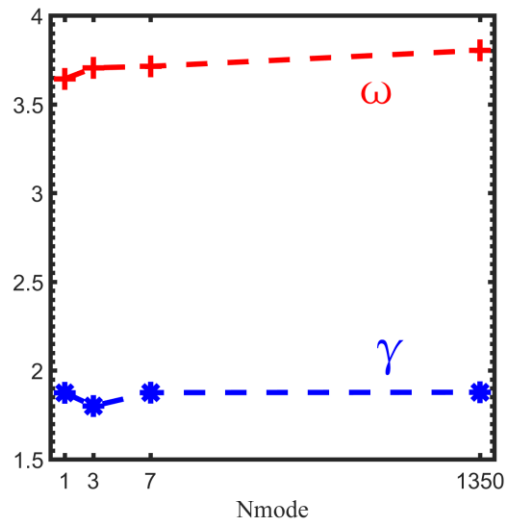


Figure 13. Growth rates (blue) and real frequencies (red) of Nmode convergence.

To study the most unstable modes in LHD, an average poloidal spectrum of diagnosis flux surface and other 10 flux surfaces, which are closest to diagnosis flux surface, is given in FIG14. The most unstable mode is around  $m_{mode}=64$  in LHD, and compared with W7-X, it is lower.

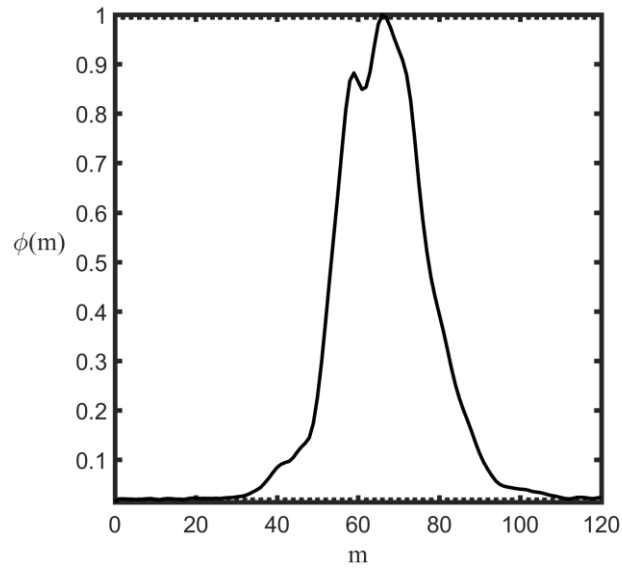


Figure 14. Averaging poloidal spectrum of different flux surfaces. X axis is mmode.

Electrostatic potential  $\phi$  on diagnosis flux surface is shown in FIG15. 3D structure of electrostatic potential on diagnosis flux surface is shown in FIG16, along with device configuration of LHD. The potential intensity shows big difference between field periods, which is similar to W7-X, but is more obvious.

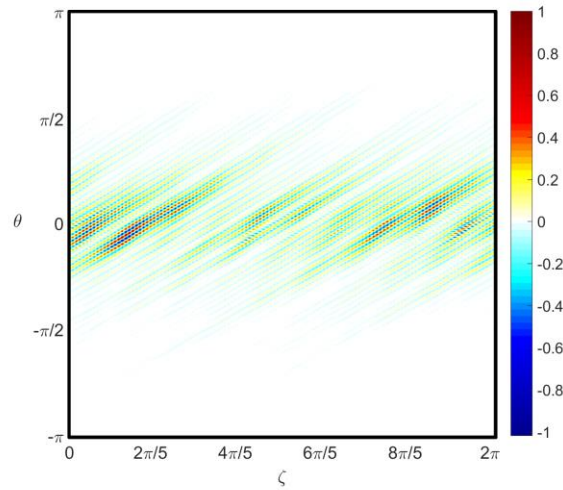


Figure 15. Phi on diagnosis flux surface. X axis is  $\zeta$ , from 0 to  $2\pi$ , and y axis is  $\theta$ , from  $-\pi$  to  $\pi$ .

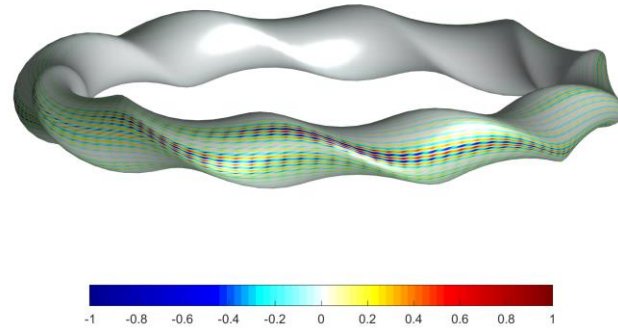


Figure 16. 3D electrostatic potential mode structure of LHD.

## V. CONCLUSION AND DISCUSSION

GTC is developed to study plasma behaviors in non-axisymmetric equilibrium configuration. Simulation results of ITG driven instabilities in W7-X and LHD using GTC are given in Section III and Section IV. Linear relation of growth rates and real frequencies of ion temperature gradient in W7-X is studied and compared with results of EUTERPE. Toroidal grids convergence of stellarators helps better understating feature of stellarators and helps future works in stellarators using GTC. Different nmodes coupling in W7-X and LHD is also studied in this article. Due to simulation results, the mode structure in W7-X is more localized, and LHD is more global and tokamak-like. The most unstable modes driven by ITG in W7-X and LHD are different, and it is higher in W7-X. The mode structure effected by mode coupling is more serious in LHD than W7-X. Future works on stellarators using GTC will be focusing on Alfven eigenmodes, like toroidal Alfven eigenmode.

## REFERENCE

- 1.Jr, Lyman Spitzer. "The Stellarator Concept." IEEE Transactions on Plasma Science 9.4(1958):130-141.
- 2.Spong, Don. "3D toroidal physics: testing the boundaries of symmetry breaking." Physics of Plasmas 22.5(2015):055602.
- 3.Helander, P, et al. "Stellarator and tokamak plasmas: a comparison." Plasma Physics & Controlled Fusion 54.12(2012):124009.
- 4.[https://www.ipp.mpg.de/4038491/017\\_12\\_2016\\_en.pdf](https://www.ipp.mpg.de/4038491/017_12_2016_en.pdf)
- 5.Fujiwara, M., et al. "Plasma confinement studies in LHD." Nuclear Fusion (1999): 1659-1666.
- 6.Nobuaki, Noda, et al. "LHD Helical Divertor and Its Performance in the First Experiments." Embo Journal 7.1(2000):197-204.
- 7.[www-naweb.iaea.org/napc/physics/FEC/FEC2012/papers/219\\_EXP703.pdf](http://www-naweb.iaea.org/napc/physics/FEC/FEC2012/papers/219_EXP703.pdf)

- 8.Kamiya, K., et al. "Observation of the inward propagation of spontaneous toroidal flow from the plasma boundary in LHD." *Physics of Plasmas* 23.10 (2016).
- 9.Kornilov, V., et al. "Gyrokinetic global three-dimensional simulations of linear ion-temperature-gradient modes in Wendelstein 7-X." *Physics of Plasmas* 11.6(2004):3196-3202.
- 10.Riemann, J., R. Kleiber, and M. Borchardt. "Effects of radial electric fields on linear ITG instabilities in W7-X and LHD." 58.7(2016):074001.
- 11.Xanthopoulos, P, et al. "Nonlinear gyrokinetic simulations of ion-temperature-gradient turbulence for the optimized Wendelstein 7-X stellarator. " *Physical Review Letters* 99.3(2007).
- 12.Helander, P, et al. "Advances in stellarator gyrokinetics." *Nuclear Fusion*55.5(2015):053030.
- 13.Ferrandomargalet, S., H. Sugama, and T. Watanabe. "Zonal flows and ion temperature gradient instabilities in multiple-helicity magnetic fields." *Physics of Plasmas* 14.12 (2007).
- 14.Nunami, M., T. H. Watanabe, and H. Sugama. "THC/P4-20 Effects of Three-Dimensional Geometry and Collisions on Zonal Flows and Ion Temperature Gradient Modes in Helical Systems." (2010).
- 15.Lin Z, et al. "Turbulent transport reduction by zonal flows: massively parallel simulations." *Science* 281.5384(1998):1835.
- 16.Hirshman, S. P., and J. C. Whitson. "Steepest-descent moment method for three-dimensional magnetohydrodynamic equilibria." 26.12(1983):3553-3568.
- 17.Dubeau, Francois, and Jean Savoie. "Periodic quadratic spline interpolation. " *Journal of Approximation Theory* 39.1 (1983): 77-88.